

## ACTIVE VIBRATION CONTROL FOR THE KAZAN ANSAT

Bastian KINDEREIT, [bastian\\_kindereit@lord.com](mailto:bastian_kindereit@lord.com), LORD Corporation (France)  
 Paul BACHMEYER, [paul\\_bachmeyer@lord.com](mailto:paul_bachmeyer@lord.com), LORD Corporation (France)  
 Alexandre BONDOUX, [alexandre\\_bondoux@lord.com](mailto:alexandre_bondoux@lord.com), LORD Corporation (France)  
 Doug SWANSON, [doug\\_swanson@lord.com](mailto:doug_swanson@lord.com), LORD Corporation (USA)  
 Anton BUSHUEV, [Bushuev\\_AA@kazanhelicopters.com](mailto:Bushuev_AA@kazanhelicopters.com), Kazan Helicopters (Russia)

### Abstract

This paper presents a high-level overview of the implementation and the results of LORD's OMNI Active Vibration Control System (AVCS) on Russian Helicopter's Ansat helicopter platform as well as a brief description of principles of the technology. The AVCS is designed so that it can be easily adapted to both existing production aircraft and new aircraft development to actively reduce in-flight vibration levels. Vibration reduction allows for increased crew comfort, reduced equipment fatigue and in certain cases even an increased flight envelope at minimal installation weight versus performance compared to other vibration reduction technologies. The technology is architected with a high degree of modularity to allow it to be adapted to a wide variety of aircraft and customer use-cases. The primary goal on the Ansat was to configure the AVCS to reduce vibration levels at the VIP seats in the aft cabin although cockpit vibration levels were also to be considered. LORD engineers worked with the Russian Helicopters team at the Kazan, Russia facility to integrate and tune the system through simulation and flight test, which resulted in reductions in vibration levels at the VIP seats of up to 84% depending on flight condition. Ultimately, these efforts resulted in two production configurations, which first appeared on a production Ansat in February 2018, making it the first Russian helicopter with LORD's Active Vibration Control technology.

### 1. PROGRAM OVERVIEW

This paper describes the joint program between LORD and the Russian Helicopters team based in Kazan, Russia to implement LORD's OMNI Active Vibration Control System (AVCS) technology onto the Ansat, a twin-engine, multi-purpose commercial-use utility helicopter.

The program presents potentially significant benefits for Russian Helicopters. With the AVCS, LORD offers a mature, reliable, lightweight and cost-effective option for significant improvements in ride comfort. Russian Helicopters hopes the improved competitiveness that integration of the AVCS will bring to the Ansat, will help them gain market share in the light twin-engine helicopter segment. This segment is presently experiencing steady growth in Russia, China, Southeast Asia, South America and Africa. Russian Helicopters has designed the Ansat with a range of use cases including emergency medical services (EMS), passenger (convertible) and VIP configurations.

#### Copyright Statement

*The authors confirm that they, and/or their company or organization, hold copyright on all of the original material included in this paper. The authors also confirm that they have obtained permission, from the copyright holder of any third party material included in this paper, to publish it as part of their paper. The authors confirm that they give permission, or have obtained permission from the copyright holder of this paper, for the publication and distribution of this paper as part of the ERF proceedings or as individual offprints from the proceedings and for inclusion in a freely accessible web-based repository.*

Production and delivery plans for the Ansat are currently projecting at least 40 helicopter deliveries per year. LORD AVCS is already certified and in use on several civil and military platforms in the rotorcraft market and integration onto the Ansat platform presents a major opportunity to enter previously untapped geographic markets. The Kazan Ansat is the first Russian Helicopter to utilize this technology.

The primary goal the Kazan team defined for the program was to improve the ride comfort at the VIP seats in the back of the cabin throughout the flight envelope, during both steady state and transient conditions. Kazan asked LORD to support an early-December 2017 deadline for the delivery of a high-performing production system in order to support the Supplemental Type Certification (STC) scheduled for later that month. The importance of the program for both companies meant both teams dedicated significant resources in ensuring the challenging performance and schedule goals were met. Today, the civilian ANSAT with the LORD AVCS is certified in Russia through an STC and has been introduced into the commercial market, with the first AVCS-equipped production helicopter completed in February 2018.

## 2. ANSAT OVERVIEW

The Kazan Ansat development began in 1995, and it was certified with a fly-by-wire system in 2004, after Ansat(-U) entered into the military (primary training) market. Since then, civilian variants of the Ansat have emerged and are looking to expand into civilian markets both inside and outside of the Russian Federation. The Ansat, as its name means in the Tatar language, is intended as a “simple and light” aircraft with a maximum takeoff weight of 3.6 tonnes. It is served by a crew of one to two and has capacity for seven to eight passengers. When fitted for medical services, it can support two stretchers and three attendants. The helicopter has a cruise speed of 220 km/h with a maximum speed of 275 km/h and a range of more than 505 km.

The Ansat main rotor consists of a four-bladed, bearingless flex beam configuration with passive pendulum absorbers fitted to each blade. This main rotor configuration was used for all phases of the flight testing campaign. It is described within this paper as “baseline” and is part of serial production of the ANSAT civil variant.



Figure 1: Kazan Helicopter Ansat (above)<sup>1</sup> and main rotor with pendulum absorber (below)<sup>2</sup>

## 3. OMNI AVCS OVERVIEW

Excessive vibrations on a helicopter airframe can cause physical and psychological discomfort to passengers and crew, fatigue and wear on components, and decreased operational capabilities of the aircraft. On many helicopters, the most prevalent and perceptible component of

fuselage vibration occurs at the main rotor blade pass frequency (equal to the number of blades times the main rotor frequency), also known as the N/rev frequency (where N is the number of main rotor blades).

The LORD AVCS is designed to suppress vibration at the N/rev frequency throughout the fuselage by cancelling dynamic loads generated by the main rotor and transmitted to the fuselage through the main rotor shaft and transmission. Force generators installed throughout the helicopter generate forces that destructively interfere with existing forces at the N/rev frequency measured at acceleration sensors (accelerometers) placed at locations throughout the aircraft where vibration control is desired.<sup>3</sup>

The OMNI variant of LORD’s AVCS is LORD’s latest generation of this technology. The OMNI system differs primarily from its predecessor, LORD’s linear AVCS, in the force generator design. The OMNI force generators (called “Circular Force Generators” or “CFGs”) generate force via co-rotating imbalance masses as opposed to sinusoidally-driven masses used in the linear force generators.

The OMNI system offers several design improvements over its predecessors, such as higher force output per weight, increased frequency range of efficient operation, and improved modularity. These design improvements maintain the underlying principles (as described above) and have a long successful pedigree in the global helicopter market stretching back to 2004. Since 2004, LORD AVC systems have logged over two million flight hours on a variety of helicopter platforms.

LORD has continued to innovate and improve the technology and the latest OMNI system offers a range of different CFG’s and interface options which has allowed for installation on a diverse range of helicopters and use cases offering vibration reductions of up to 90% over baseline.

### 3.1. Architecture

The AVCS is designed to maximize adaptability through a modular architecture, which allows LORD engineers to choose from several different CFG and accelerometer variants to meet the specific performance requirements or physical constraints specific to the customer in question.

An AVCS consists of a Central Controller connected to up to twelve CFG’s and fourteen accelerometer sensors. In practice, typically not all

<sup>1</sup> References [4]: Russian Helicopters, JSC. (2018)

<sup>2</sup> References [1]: Heli-Russia (2017)

<sup>3</sup> Ref [2]: Mahmood, R. et al., ‘In-flight Demonstration of Active Vibration Control Technologies on the Bell 429 Helicopter’

the available channels are used. The CFG's and accelerometer sensors are often installed on primary structural elements under the floor, which tend to be the primary transmission paths of the rotor-induced vibration. This is the case on the Kazan Ansat as well.

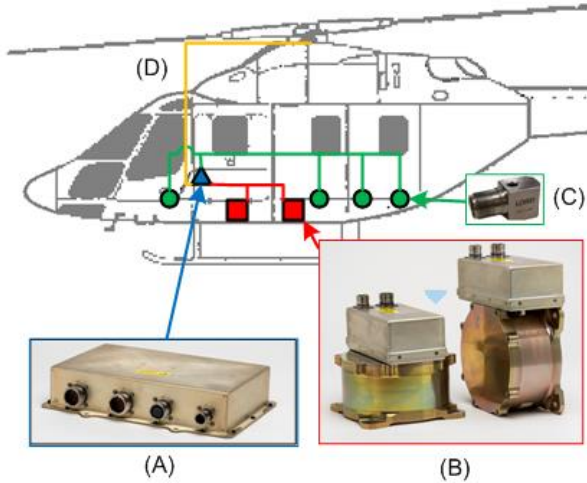


Figure 2: OMNI AVCS Diagram<sup>4</sup>

This architecture allows the systems engineers to target specific areas of the fuselage for vibration attenuation. For example, in the case of the Ansat, the aft cabin where the VIP seats are located was a primary focus and installation locations were chosen accordingly.

The CFG's force magnitude and force phase are independently controlled by a Central Controller. The calculated commands are based on a closed-loop cost-minimization algorithm using the N/Rev vibration component represented in complex form as the error to reduce. The complex value representing the error is measured by the control accelerometers multiplied by a channel-specific, user-defined weighting. Also considered is a user-defined weighting on CFG effort as the cost or error to be minimized.

In order to extract the N/Rev component from the control accelerometer signals, the Central Controller must continuously determine what the real-time N/Rev frequency and phase value is. The Central Controller determines this using a tachometer signal which is processed using a number of user-settable parameters.

The emphasis on a modular approach extends beyond the physical architecture to the software architecture as well. Both the Central Controller and the CFG's have their own LRU-specific

<sup>4</sup> LRU's are shown in Figure 2 where (A) is the OMNI Central Controller, (B) is two variants of the OMNI CFG, (C) is a variant of the control accelerometers and (D) is the tachometer input signal to the Central Controller.

application software, which is independent of the helicopter platform. The LRU performance parameters to meet platform-specific operational requirements are defined in a separate, field-loadable software file called a Parameter Data Item File (PDFI). This allows LORD to work with the customer to tailor the system behavior using a set of tuning parameters to meet a wide range of requirements, without modifying the underlying logic embedded in the application file.

### 3.2. CFG Overview

The CFG's generate circular forces by controlling two independent imbalance masses that spin at the N/rev blade pass frequency. Both imbalance masses spin in the same direction. Each imbalance mass creates a rotating force vector equal to the product of its imbalance authority ( $mr$ ) and the square of its angular velocity.<sup>5</sup> The force vectors of the two rotating imbalance masses resolve into a single force vector as described in equation (1) and described pictorially in Figure 3.

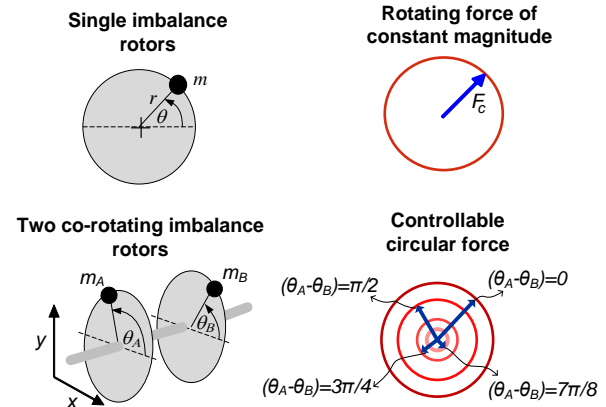


Figure 3: Circular Force Generation Depiction

$$(1) F_C = m_A r_A \dot{\theta}_A^2 e^{j\theta_A} + m_B r_B \dot{\theta}_B^2 e^{j\theta_B}$$

Where:

- $F_C$  = resultant force vector of both imbalance masses
- $m_A, m_B$  = mass of imbalance mass
- $r_A, r_B$  = moment arm of imbalance mass c.g
- $\theta_A, \theta_B$  = angular position of imbalance mass

The imbalance mass control is handled by the CFG itself, which receives the force frequency, force magnitude, and force phase commands from the Central Controller and translates them into the appropriate motor commands to control the imbalance masses. Having the imbalance mass

NOTE: Actual LRU locations are defined in Figure 7 and Figure 8

<sup>5</sup> References [5]: Swanson, D. et al., 'Active Vibration Control Using Circular Force Generators'

command logic handled by the CFG itself allows for easy interchangeability of CFG's in the system since the commands the Central Controller sends are independent of the CFG variant. This flexibility allowed LORD to use three different CFG part numbers on the Ansat configuration to accommodate space constraints. On the Ansat, both a three- and a four-CFG configuration were chosen for production.

Further details of the OMNI CFG's can be found in Reference [5].

### 3.3. Error Sensing

Error sensing for the closed-loop control algorithm is handled by accelerometers. The Central Controller determines the in-phase and quadrature components at the N/Rev frequency of each of the accelerometer signals by demodulating them using the tachometer frequency input to the Central Controller to determine the instantaneous N/Rev frequency.

The accelerometers are placed in locations, which, when N/Rev vibration at that location is attenuated, will result in the desired vibration control effect. The primary goal of the Ansat program was to improve the ride comfort of the VIP passengers in the aft cabin. As such, accelerometers were placed on the main structural members to which the VIP seats were bolted.

The three- and four-CFG Ansat production configurations used nine and eleven accelerometer channels respectively, out of an available fourteen channels.

### 3.4. System Model

The control loop plant is a three-dimensional matrix of complex values called the "SYSID". The SYSID defines the transfer functions between each CFG and each accelerometer and is generated through an automated procedure called "System Modeling". During this procedure, each CFG is sequentially stepped through a set of frequencies (called "Frequency Bins"). These frequencies cover the N/Rev operating range of the helicopter with some margin on either end of the range. At each of these frequencies, the CFG will dwell for a specified time while generating a fixed commanded force. During the dwell at each frequency, the Central Controller determines average in-phase and quadrature values for each accelerometer channel for the CFG outputting force and stores the value at the proper element location in the SYSID matrix. The sequence allows the Central Controller to determine a transfer function between every

accelerometer-CFG pair, at every bin frequency. At the end of the procedure, the SYSID will have the following number of transfer functions:

$$(2) n_{Act} n_{Acc} n_{Bin} = n_{TF}$$

Where:

$n_{Act}$  = Number of CFG's

$n_{Acc}$  = Number of Accelerometers

$n_{Bin}$  = Number of Frequency Bins

$n_{TF}$  = Number of Transfer Functions

Each of the parameters defining the procedure (frequencies, dwell time and force) is set in the Central Controller PDIF designed for the helicopter.

The frequency bins account for frequency-dependence of the transfer functions which testing has demonstrated is non-negligible. Force-dependence of the transfer functions is assumed to be negligible at sufficiently large forces. The SYSID force magnitude is generally determined using a combination of linearity testing on ground and observation of typical force outputs during flight.

Concerns for the distorting effects the weight-on-wheels boundary condition could have on the transfer function measurements for on-ground System Modeling have led LORD to explore taking the transfer functions in-flight using a technique called "Off NR" System Modeling.<sup>6</sup> The reason System Modeling is typically performed on the ground is to avoid having the vibration signal from the helicopter rotor (the N/rev frequency vibration content the AVCS is designed to suppress) interfere with the transfer function measurement. This can be avoided on a variable rotor speed helicopter by taking the transfer function at frequencies sufficiently far from the current operating frequency such that the disturbance from the operating frequency will be sufficiently attenuated as to be negligible. As the CFG operating frequency moves to the next bin, the pilot must change the helicopter rotor frequency as well in order to maintain a sufficient frequency difference.

### 3.5. Closed-Loop Control

The SYSID, or control loop plant, discussed in section 3.4, is stored in non-volatile memory and used by the control algorithm to compute the cost-minimization gradient.

As the N/rev frequency changes, the algorithm adjusts its plant model accordingly based on an interpolation of the two nearest bins thereby

<sup>6</sup> References [3]: Monaco, M. et al., 'Achieving Near Zero N/Rev Vibration with Zero-Vibe™ Technology'

maintaining a high degree of plant accuracy.

LRU placement, along with CFG spin direction, has a significant impact on convergence, stability and steady-state error, and LORD has developed several techniques to employ during the flight testing phase of the program to optimize these parameters, which are further discussed in 4.2.

### 3.6. Installation and Interface

In addition to the primary vibration control functions discussed above, LORD has designed in a number of different ways to integrate the system onto a helicopter.

The AVCS can be controlled via discrete inputs that can map cockpit switches to various functions. The most commonly mapped function in a production configuration is the initialization of the system modeling procedure, but can also include force neutralization or CFG spin-down among others.

The Central Controller also has a set of relays that can be mapped to various internal variable states using the PDIF. These relays are connected to pins on external connectors and can in turn be connected to cockpit indicator lights. These lights then reflect the state of the mapped internal variables and can thusly be used to indicate fault status, system state, or the state of a number of other variables.

The AVCS also provides an external interface for ARINC or RS-422 communication. These protocols offer the additional benefit of two-way communication. This means that control and real-time monitoring can be handled in this single interface along with integrated data-logging functionality.

Figure 4 shows a schematic of the AVCS as installed on the Ansat. The two configurations selected for production are the same as far as the schematic interconnects except for the number of CFG's and accelerometers. The number in parentheses indicates the number of that component that is present on the Ansat AVCS. The "(3/4)" in the "CFG" label indicates the first configuration has three CFG's and the second configuration has four CFG's. The "(9/11)" in the "ACC Inputs" accelerometer label indicates that the first configuration uses nine control accelerometers and the second configuration uses eleven. On the Ansat, the Kazan team has chosen to use only one Discrete Input, which is used to initiate the system modeling procedure. The four relay lights are mapped to indicate power and LRU fault status.

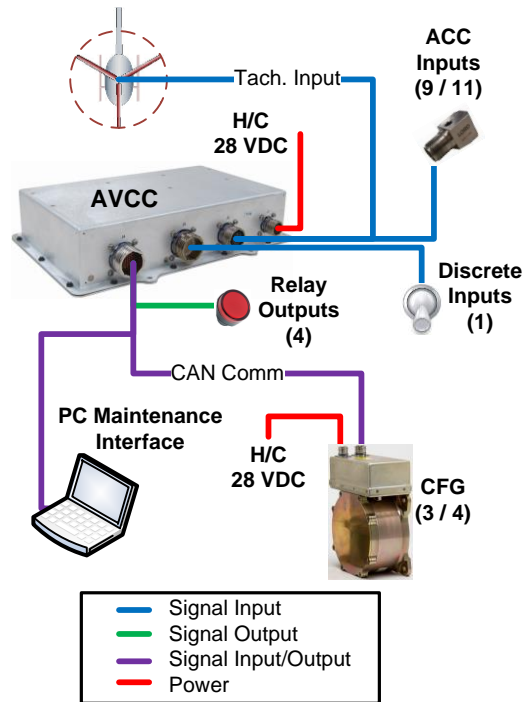


Figure 4: Production Ansat AVCS integration schematic<sup>7</sup>

## 4. ANSAT INTEGRATION AND TUNING

### 4.1. Integration

The program was divided into three main phases. The goal of the first phase was to determine the viability of an AVCS solution as a means to address the concerns Kazan had regarding the vibration levels at the VIP seats on the Ansat. Additionally, Phase I activities included taking ground-based transfer functions with linear- and OMNI-based systems installed above the floor. A baseline flight was also performed with accelerometers installed throughout the fuselage to collect data to be used as inputs for the simulation work in Phase II.

During Phase II, LORD worked with the Kazan team to determine possible CFG mounting locations. Using these locations in conjunction with the Phase I data, LORD ran simulations to determine which locations showed the most promise for Phase III, the flight test phase, and what level of results could be expected.

With the Phase II outputs, LORD and the Kazan team determined where to mount candidate CFG's and accelerometers for the Phase III flight test. The output of the on-site, flight testing portion of Phase III was a preliminary production configuration with the CFG locations and spin directions defined

<sup>7</sup> There are two production configurations which account for the two numbers for the Accelerometer (ACC) and CFG channels

along with the accelerometer locations. After flight test, LORD and Kazan completed Phase III by defining the final details of the configurations such as the helicopter interfaces and serialization activities related to logistics, configuration management etc.

#### 4.2. Flight Testing and Optimization

Test asset constraints resulted in a very compressed flight test schedule in early July 2017. LORD provided on-site support for the initial system installation, which took roughly a week. This was followed by another week of actual flights.

In order to maximize the number of candidate accelerometer locations, a second Central Controller was employed, with a second set of accelerometers.

Additionally, there were nine initial CFG candidate locations with three different CFG variants depending on the installation constraints of the location in question.

Cost and weight targets dictated that the final system design should be a three- or four-CFG system, and previous program experience suggested that something around ten accelerometers would be appropriate depending on results.

Transfer functions between each accelerometer channel and each of the CFG channels were taken with the CFG's spinning in one direction, then a second set was taken with the CFG's spinning in the other direction. Figure 5 shows an example of transfer functions between a single CFG and three accelerometer channels, with the clockwise transfer function indicated by "CW" and the counter-clockwise transfer function indicated by "CCW". As the figure shows, the spin direction can have a tremendous impact on the transfer function phase and magnitude.

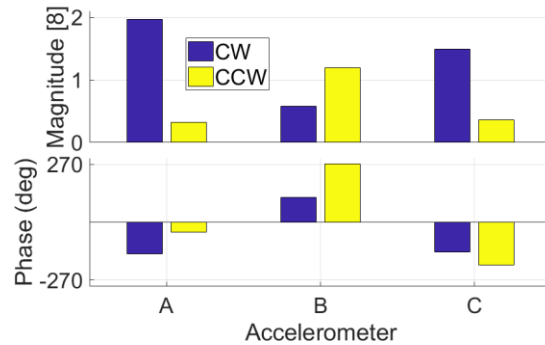


Figure 5: CFG Spin Direction Effect on Transfer Function<sup>8</sup>

With system modeling complete, the Kazan flight test team then performed a baseline flight during which the critical flight conditions were flown with the AVCS off but operating in data collection mode.

With this data, LORD was able to determine a candidate flight test configuration to test on the next flight using simulation techniques discussed below.

Using the transfer functions captured in the SYSID's, LORD selected a subset of accelerometers based on how they scored on three criteria:

- First, they had to be near the VIP seat as these were most likely to correlate with VIP passenger comfort.
- Second, the set of accelerometers had to be likely to yield a SYSID that would result in a balanced convergence with a low steady-state error, which LORD can predict by looking at various characteristics of the matrix. Since the CFG's had not yet been selected, let alone their spin-direction, this had to be done using a probabilistic approach. That is to say, the set that was picked was more likely than the others to exhibit good characteristics given a random set of CFG's and spin directions.
- Third, accelerometers were selected for which there was a large number of CFG's with a high authority over that location.

With a candidate accelerometer set chosen, the next task was to define the CFG channel and spin-direction subset from the candidate locations. As was previously mentioned, the number of CFG's was already targeted to be three or four based on the business case.

A brute force approach was employed for the simulation step in which a composite SYSID was

<sup>8</sup> Transfer function magnitude has been normalized

constructed for every combination of three CFG's and then four CFG's out of the superset of CFG's. Then, a composite SYSID for every spin permutation for each of those combinations was generated. The equation for the total number of simulations for each accelerometer subset and CFG number combination is shown in equation (3).

$$(3) \binom{n_{Act}}{k} * 2^k * n_{fc} = n_{cm}$$

Where:

- $n_{Act}$  = Number of Candidate CFG's
- $k$  = Number of CFG's in Target Configuration
- $n_{fc}$  = Number of Flight Conditions
- $n_{cm}$  = Number of SYSID's

A simulation was run for each of these SYSID's using the vibration data from the baseline flight for each flight condition to predict the steady-state and transient performance of each system model.

Each result was evaluated based on error magnitudes at each of the flight conditions. The SYSID from the winning result dictated the CFG locations to use, as well as their spin directions. These parameters were then written into the Central Controller PDIF to be used on the next flight.

An example of the process results is shown in Figure 6. The "AVC Off" curve shows the mean of the magnitudes of the complex array of the control accelerometers' vibration levels. This array is generated for each flight condition with the AVCS neutralized. This is the aforementioned "baseline flight" data used as an input to the simulation along with the composite SYSID.

The prediction for the highest-scoring SYSID is shown by the "Predicted Best Config" curve in Figure 6. This configuration was then flown in the next flight and the results are shown in the "Flight Data from Predicted Best Config" curve in Figure 6. The actual data shows acceptable agreement with the prediction save for a single flight condition (excluding the outlier, the average error is approximately 8%). Outliers can sometimes occur particularly when the "AVC Off" data is taken from a different flight on a different day as was the case here. The consequence is that different inputs are used in the simulation versus the actual inputs the AVCS sees during the flight, so some variance is expected. Finally, to demonstrate the impact the configuration can have on performance, the worst performing simulation results are shown in Figure 6 with the curve labelled "Predicted Results of Worst Config". In the worst configuration, it is predicted the AVCS will offer only a about an average fifteen percent improvement over baseline over the flight envelope whereas the best

configuration offers around a seventy-seven percent reduction over the baseline averaged over all control accelerometers.

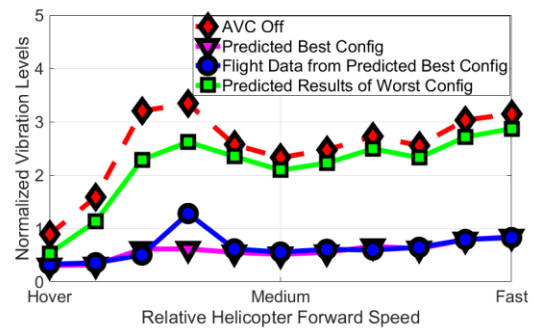


Figure 6: All Control Accelerometer Simulation Results Example

Ultimately, the most important criterion on which to measure program success is the subjective feeling of the crew and passengers. Proper selection of the control accelerometer locations plays a critical role in successfully achieving good subjective performance. If the measured vibration is not well correlated to the human sensation, the AVCS controlling vibration at that location will not necessarily result in improved comfort. Therefore, after each flight, LORD re-evaluates which accelerometers to enable as control accelerometers based on the crew feedback and measured data. To determine which accelerometers to enable, each channel is evaluated to see if it is predicted to yield both good correlation to the subjective feeling of the occupants and if the control accelerometer set will yield good simulation results.

In addition to focusing on bringing the VIP seat area vibration levels down, a secondary requirement of the program was to reduce cockpit vibration levels, or at least not exacerbate them.

Over the course of the campaign, it was determined that to achieve significant results in the cockpit, a fourth CFG and modified CFG locations, as well as additional control accelerometers in the cockpit area would be necessary.

Ultimately, Kazan selected two configurations for production. The first was a three-CFG system with very good VIP seat performance but only mildly better cockpit performance over baseline. The second configuration was a four-CFG system with comparable VIP performance with respect to the three-CFG configuration, but much improved cockpit performance.

## 5. PRESENTATION OF RESULTS

As discussed in section 4.2, over the course of the flight test campaign, Kazan decided to focus on two different configurations for a production solution. The major difference between the two configurations ultimately selected for production was the cockpit performance. The four-CFG configuration achieved significantly better performance in the cockpit and VIP areas over baseline while the three-CFG configuration achieved significant improvement in the VIP area over baseline but only mild improvement over baseline in the cockpit area. Production CFG locations are shown in Figure 7 and accelerometer locations are shown in Figure 8.

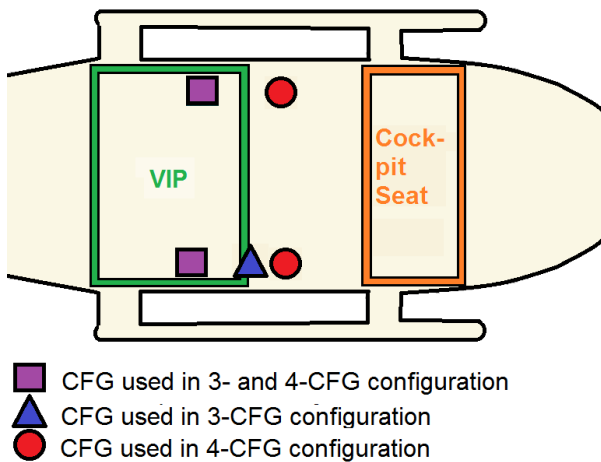


Figure 7: Production CFG Locations

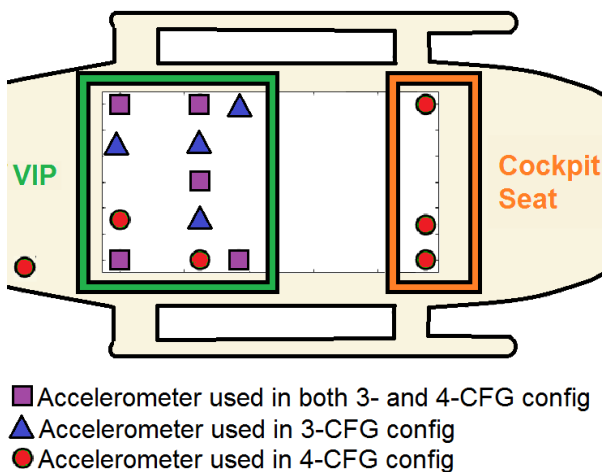


Figure 8: Production Accelerometer Locations

### 5.1. Steady State Results

As the helicopter spends the vast majority of a typical flight at a select number steady state conditions (e.g. constant cruise speed), good steady state AVCS performance at those flight conditions is crucial.

Typically, during a flight test, speeds from hover to maximum level flight speed ( $V_h$ ) are flown along with intermediate speeds at regular intervals. Time permitting, during each of these flight conditions, vibration levels with the AVCS neutralized are measured, and then again with the AVCS enabled.

Although around a dozen steady state flight conditions were taken for each flight, as previously mentioned, there are a few speeds that may be given more consideration in the evaluation of the configuration and in the interest of brevity, only the results from these speeds are shown.

The vibration data on which the configurations were judged were collected by two categories of accelerometers for the purposes of the flight test. The control accelerometers made up one category and were all connected to the primary Central Controller which was controlling the CFG's. Control accelerometers provide the error data input to the control algorithm and consequently, the AVCS tries to attenuate vibration only at the control accelerometer locations. In addition to the control accelerometers, a second Central Controller was installed where all the channels were dedicated to monitoring accelerometers. These accelerometers record vibration data but were not considered in the control algorithm. The channels on the primary Central Controller not dedicated to control accelerometers were used as monitoring accelerometer channels. Due to cost and weight considerations, production configurations only employ control accelerometer channels. The monitoring accelerometers served two purposes. The first was to measure the impact of the configuration under consideration on the uncontrolled parts of the cabin. Additionally, the monitoring accelerometers could be changed to control accelerometers in subsequent flights should the optimization discussed in section 4.2 show that enabling that channel could yield positive results.

For the grouped bar plot results in Figure 9 and Figure 10, the focus was on showing how well the AVCS did its primary job, namely to reduce error (i.e. vibration at the control accelerometers). Therefore, the results focus solely on the control accelerometers.

In Figure 9 and Figure 10 below, the vibration magnitude of each control accelerometer in the AVC On state (when the AVCS is working to control vibration) was normalized against the magnitude from the same location and flight condition in the baseline state with the AVCS neutralized. So, for example, a bar plot value of 40% indicates that the vibration level with the AVCS enabled is 40% of the level when the AVCS is neutralized. These normalized values were then averaged together for

the area in question (VIP or cockpit) to produce the values displayed in the plots. The one exception is the plot of the cockpit accelerometers in the three-CFG configuration. As there are no control accelerometers in the cockpit in the three-CFG configuration, data from the monitoring accelerometers at the same locations as the four-CFG cockpit control accelerometers were used.

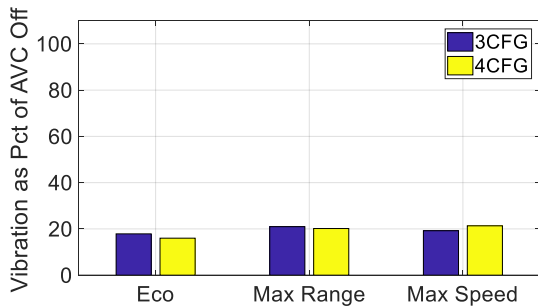


Figure 9: Steady State VIP Control Accelerometers

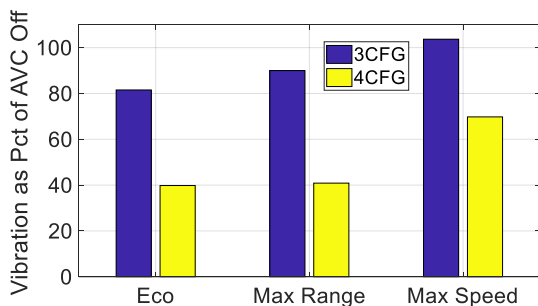


Figure 10: Steady State Cockpit Control Accelerometers<sup>9, 10</sup>

Figure 9 shows very strong performance for both the three- and the four-CFG configurations for the VIP control accelerometers with no clear advantage for either one. However, Figure 10 shows a very clear advantage for the four-CFG configuration for the cockpit control accelerometers whereas there is only a mild reduction in vibration for the three-CFG configuration.

While the grouped bar plots show the ability of the AVCS to reduce error at the control accelerometer locations, broadening the set of accelerometer data under consideration can show if the control accelerometers were properly selected (the importance of control accelerometer location is discussed in section 4.2). To do this, the contour plots displayed in Figure 11 through Figure 14 show the results from *all* of the accelerometers in the region of interest, be they control

accelerometers or monitoring accelerometers. Occasionally, while the AVCS does a good job of attenuating vibration at the control accelerometer locations, it can sometimes have only a minor impact or even exacerbate vibrations in other locations. Such a situation can negatively affect the correlation between the error measured at the control accelerometers, and the subjective feeling of the passengers and crew. This, in turn, negatively affects the ability of the AVCS to improve ride comfort, regardless of how effective it is at reducing error at the control accelerometers.

Furthermore, the grouped bar plots show the AVC On, controlled vibration level as a percentage of its own baseline value. This can be good for showing the relative impact of the AVCS. Ultimately though, what matters to the crew and passengers, is the absolute vibration level. The contour plots do a better job of communicating this because the vibration levels are all normalized against a single, common baseline value. So, for example, Figure 10 suggests the AVCS didn't do quite as good a job at reducing cockpit vibration levels as VIP vibration levels shown in Figure 9. While true, since the baseline cockpit vibration levels were lower than the baseline VIP levels, the AVC On levels in the cockpit were not as bad as the grouped bar plots would suggest. This is communicated more accurately in the contour plots.

For the contour plots, the regions of interest were the area surrounding the VIP seats towards the back of the fuselage, and the pilot and co-pilot seats in the cockpit. The same three speeds selected for Figure 9 and Figure 10 were selected for the contour plots in Figure 11, Figure 12 and Figure 13. A similar pattern emerged with the contour plots as compared to the grouped bar plots. The performance over baseline in the VIP area was strong for both configurations, with good cockpit performance for the four-CFG configuration, but only mild improvements in the cockpit for the three-CFG configuration.

<sup>9</sup>For the three-CFG data, since there are no control accelerometers in this configuration, data from the monitoring accelerometers at the four-CFG configuration cockpit control accelerometers were used.

<sup>10</sup> Although Figure 10 would seem to suggest vibration is worse in the cockpit than the VIP levels shown in

Figure 9, one reason the VIP area was prioritized was because the baseline levels were higher. This can be more readily observed in the contour plots (Figure 11, Figure 12, Figure 13 and Figure 15) which are all normalized against a single value

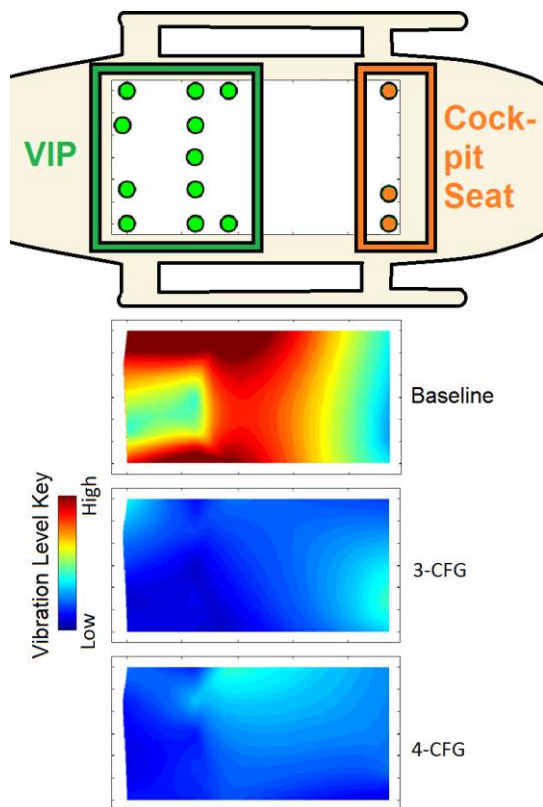


Figure 11: Eco, Steady State

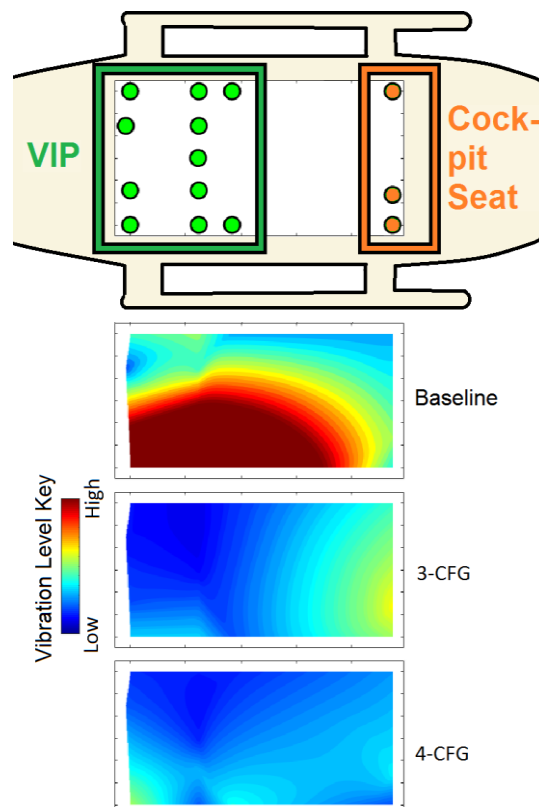


Figure 13: Max Speed, Steady State

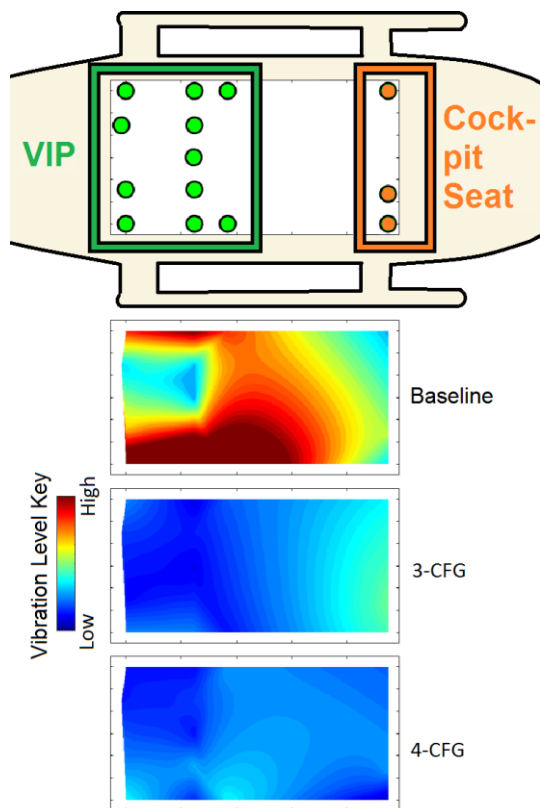


Figure 12: Max Range, Steady State

Overall, the steady state results showed very good performance. Although only three flight conditions are shown, the other flight conditions showed similar or in some cases better performance. Furthermore, the contour plots show that the placement of the AVCS control accelerometers have a positive impact locally to their position and throughout the entire VIP area and cockpit.

## 5.2. Transient Results

The transient flight condition that typically creates the most discomfort to the crew and passengers is flare. This maneuver is performed to slow the helicopter during the landing approach and results in some of the highest observed vibration levels. Additionally, the fact that this maneuver needs to be performed at least once per flight contributes to the importance of controlling vibration for this particular transient flight condition.

Flares can exhibit large variance in measured vibration even when performed back-to-back. The variability in the flare vibration profile can be influenced by a number of factors such as the helicopter configuration (e.g. prototype versus production), weight configuration, pilot and atmospheric conditions. The flares for the two configurations discussed in this paper were performed on the same helicopter by the same

crew but on different days and at different fuel loads.

The large expected variance in vibration input from flare to flare, and the limited sample size taken during this flight test campaign should be considered for the confidence level of any conclusions drawn from looking at the data.

To condense the results for presentation, a time-wise mean of all the enabled VIP accelerometers and another for all the cockpit seat accelerometers enabled in the four-CFG configuration was taken for both the AVC On condition, as well as the baseline condition for the three-CFG configuration. This process was repeated with the four-CFG configuration.

The time at which this time-wise mean reached a maximum was then determined both for the AVC On and the baseline data, and the region average was calculated (i.e. the average of all the cockpit control accelerometers, and the average of all the VIP control accelerometers at the time at which the average of all control accelerometers reached its maximum).

The magnitude of the AVC On condition was then compared to the baseline condition for each region and the results are displayed in Figure 14.

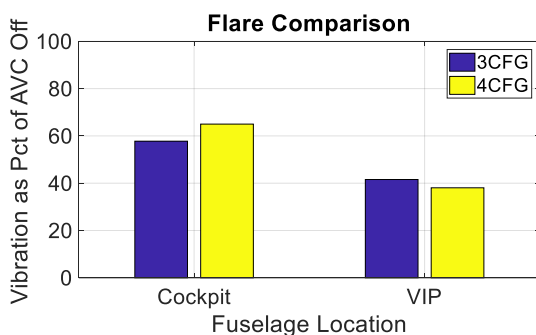


Figure 14: Configuration Comparison for Flare by H/C Region

The figure shows that, contrary to the results in the steady state flight conditions, the four-CFG cockpit performance was slightly degraded with respect to the three-CFG configuration, whereas the VIP was improved.

For the contour plots, the same approach was taken as with steady state where all the accelerometers in the region of interest (VIP and cockpit seat), be they control or monitoring, were considered to verify that the control accelerometers were well chosen.

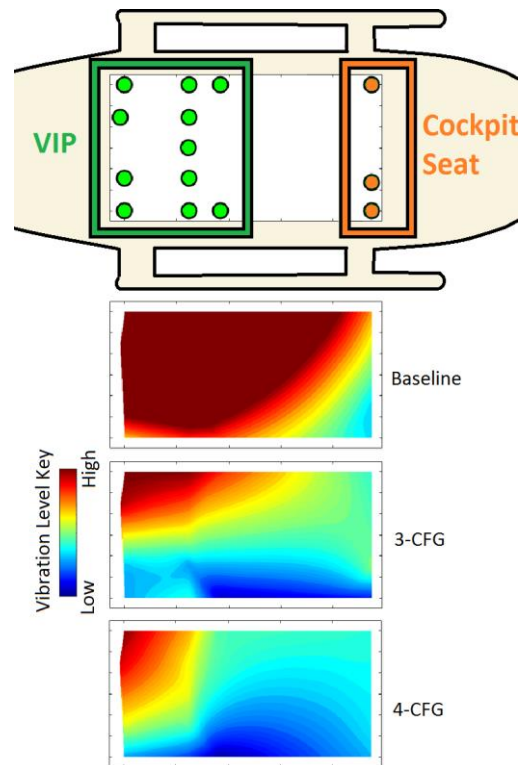


Figure 15: Flare<sup>11</sup>

Flare contour plot results showed a small but noticeable edge for the four-CFG configuration along with a slight improvement on the left side of the VIP area.

The flare performance criterion was not given as much weight as steady state performance because of the much more significant duration of steady state flight versus flare during a typical flight profile. The goal was to find the best steady state configuration and then to confirm that it had acceptable flare performance. Therefore, while some configurations which were not selected for production had better performance during flare, the production configurations were deemed to be the optimal compromise when considering the importance granted to each region and each flight condition.

## 6. PHASE III CLOSURE

With the LRU locations and CFG spin directions selected for serialization, activities to close out Phase III and the development stage of the program took place over the next few months to meet the Kazan production and certification deadlines.

On the technical side, this mainly involved interface integration, which was a significant collaborative

<sup>11</sup> Due to vibration levels during flare being so much higher than during steady state flight conditions, the

saturation threshold in the flare contour plots was twice as high as in the steady state contour plots

effort between the two engineering teams. Much of the effort was involved in working with the Kazan team to integrate the AVCS into the production fuselage and to assist in the design of the harness and Central Controller PDIF to ensure proper cockpit display of system status and power severe functionality.

Finally, a successful software SOI4 audit by the Kazan engineering team at LORD France's Lyon offices was conducted to lead into a type certification by the Russian airworthiness authorities, clearing the way for the first production installation in February 2018.

## 7. CONCLUDING REMARKS

The results of the production configurations over baseline showed a significant improvement at the VIP seats both from a quantitative standpoint, as measured by accelerometer measurements, as well as a qualitative standpoint based on crew and passenger feedback.

Steady state cockpit improvements offered by the four-CFG system are clearly beneficial to the pilots, but may also have an indirect benefit for the passengers. Reduced pilot fatigue may expand the flight envelope, and allow the pilot to perform his task safely and effectively.

If, on the other hand, the end-user prioritizes weight and cost, the three-CFG configuration may be the optimal solution.

With ride comfort benefits from the successful integration of AVCS, the Ansat offers a very competitive option for the growing twin-engine helicopter market. The diverse roles of the Ansat beyond VIP, as well as the other Russian Helicopters platforms suggest a range of promising opportunities for future collaboration between the two companies.

## 8. REFERENCES

[1] Heli-Russia (2017), Russian Helicopter Exposition, Kazan Ansat floor model, Photo taken by LORD Corporation.

[2] Mahmood, R., Heverly, D., "In-flight Demonstration of Active Vibration Control Technologies on the Bell 429 Helicopter", American Helicopter Society International Forum, 2012, Fort Worth, Texas USA

[3] Monaco, M., DiOttavio, J., Kekaley, D., "Achieving Near Zero N/Rev Vibration with Zero-Vibe™ Technology", AHS International Forum, 2018, Phoenix, Arizona USA

[4] Russian Helicopters, JSC. (2018), Ansat technical page. Retrieved from <http://www.russianhelicopters.aero/en/helicopters/civil/ansat/photo>.

[5] Swanson, D., Black, P., Girondin, V., Bachmeyer, P., Jolly, M., "Active Vibration Control Using Circular Force Generators," 41st European Rotorcraft Forum Proceedings, Munich, Germany, Sept. 2-5, 2015